Suppl. Table S1

Twenty glycan structures on the glycan array.

No	Names	Glycan-structures	No	Names	Glycan-structures
1	Tn	α-GalNAc-R*	11	Blood type-A disaccharide	GalNAcα1-3Galβ-R
2	Thomsen–Friedenreich (TF)	Galβ1-3GalNAcα-R	12	Blood type-B disaccharide	Galα1-3Galβ-R
3	6'Sia-Tn	Neu5Acα2-6GalNAcα-R	13	3'Fuc-Gal	Fucα1-3Galβ-R
4	3'Sia-Tn	Neu5Acα2-3GalNAcα-R	14	Type-2 3'Sia-LacNAc	Neu5Acα2-3Galβ1-4GlcNAcβ-R
5	3'Sia-TF	Neu5Acα2-3Galβ1-3GalNAcα-R	15	Type-2 LacNAc	Galβ1-4GlcNAcβ-R
6	Lewis a	Galβ1-3(Fucα1-4)GlcNAcβ-R	16	Type-1 3'Sia-LacNAc	Neu5Acα2-3Galβ1-3GlcNAcβ-R
7	Type-1 LacNAc	Galβ1-3GlcNAcβ-R	17	Type-2 6'Sia-LacNAc	Neu5Acα2-6Galβ1-4GlcNAcβ-R
8	Lewis x	Galβ1-4(Fucα1-3)GlcNAcβ-R	18	hyaluronic acid	—
9	3'Sia-Lewis-a	Neu5Acα2-3 Galβ1-3(Fucα1-4)GlcNAcβ-R	19	heparan sulfate	—
10	3'Sia-Lewis-x	Neu5Acα2-3 Galβ1-4(Fucα1-3)GlcNAcβ-R	20	chondroitin sulfate sodium salt	—

Suppl. Table S2

Quantitative glycan-array binding signals of hRTL-1 to hRTL-6.

No	Glycans	hRTL-1	hRTL-2	hRTL-3		hRTL-4	hRTL-5	hRTL-6
1	Tn	67.39 ± 2.38	117.27 ± 2.80	8.13 ± 0.40		3.72 ± 0.37	8.11 ± 0.45	49.44 ± 1.66
2	Thomsen–Friedenreich	322.73 ± 5.63	444.55 ± 3.72	30.27 ± 1.94		26.11 ± 0.73	267.93 ± 3.91	457.19 ± 1.09
3	6'Sia-Tn	11.31 ± 0.22	6.26 ± 0.56	4.59 ± 0.28		4.95 ± 0.32	6.51 ± 1.07	19.90 ± 0.67
4	3'Sia-Tn	88.78 ± 3.64	84.06 ± 0.71	7.28 ± 0.58		6.30 ± 0.12	8.35 ± 0.79	31.46 ± 1.75
5	3'Sia-TF	262.25 ± 6.21	297.39 ± 6.04	26.59 ± 2.23		22.38 ± 1.50	65.42 ± 3.64	137.50 ± 2.19
6	Lewis a	10.06 ± 0.52	4.98 ± 1.02	2.68 ± 0.13		2.75 ± 0.07	5.67 ± 0.69	18.76 ± 1.02
7	Type-1 LacNAc	353.46 ± 10.90	440.49 ± 5.20	26.47 ± 2.69		32.56 ± 5.79	503.46 ± 10.15	628.48 ± 0.36
8	Type-2 Lewis x	7.54 ± 0.23	1.35 ± 0.59	1.74 ± 0.17		0.58 ± 0.42	4.97 ± 0.39	21.76 ± 0.96
9	Type-1 3'Sia-Lewis-a	9.81 ± 0.67	0.17 ± 0.25	0.55 ± 0.25		2.22 ± 0.40	2.21 ± 0.14	17.18 ± 0.39
10	Type-2 3'Sia-Lewis-x	3.12 ± 1.70	0.24 ± 0.20	1.66 ± 0.70		1.28 ± 0.39	0.45 ± 0.37	20.74 ± 0.67
11	Blood type-A disaccharide	76.43 ± 8.13	175.62 ± 10.67	12.21 ± 1.07		12.93 ± 0.69	107.78 ± 0.35	619.39 ± 3.35
12	Blood type-B disaccharide	185.53 ± 8.52	273.72 ± 7.58	16.06 ± 0.95		14.09 ± 0.57	33.01 ± 0.87	361.28 ± 4.55
13	3'Fuc-Gal	43.65 ± 2.74	87.50 ± 1.43	4.28 ± 0.31		3.41 ± 0.56	4.80 ± 0.60	33.92 ± 2.11
14	Type-2 3'Sia-LacNAc	22.86 ± 4.54	12.84 ± 0.64	2.83 ± 0.30		3.60 ± 0.62	11.89 ± 1.29	39.13 ± 3.14
15	Type-2 LacNAc	86.70 ± 5.14	248.63 ± 1.85	10.08 ± 1.06		6.99 ± 0.80	198.16 ± 12.26	334.99 ± 14.55
16	Type-1 3'Sia-LacNAc	211.27 ± 11.49	254.05 ± 2.50	14.29 ± 2.04		10.21 ± 1.33	200.79 ± 16.17	238.62 ± 15.25
17	Type-2 6'Sia-LacNAc	4.34 ± 0.64	0.15 ± 0.21	0.76 ± 0.31		0.05 ± 0.08	1.70 ± 0.78	11.25 ± 1.30
18	hyaluronic acid	0.74 ± 0.20	1.15 ± 0.41	0.00 ± 0.00		0.00 ± 0.00	0.81 ± 0.26	0.32 ± 0.45
19	heparan sulfate	0.23 ± 0.33	2.03 ± 0.67	0.48 ± 0.59		2.25 ± 0.50	0.00 ± 0.00	22.23 ± 1.01
20	chondroitin sulfate	1.16 ± 0.73	1.42 ± 0.52	0.56 ± 0.31		3.19 ± 0.31	0.49 ± 0.19	30.67 ± 2.78

The table caption is on the next page.

Fluorescence intensities are presented as the mean ± SD from three replicate spots (n = 3) for each glycan. Glycan-array analysis was performed using each hRTL at a concentration of 100 μg/mL. Net fluorescence intensities were obtained after background subtraction. Relative fluorescence intensities (%) were calculated as the ratio of the mean net fluorescence intensity for each glycan to the mean fluorescence intensity of the immobilized Cy3-labeled bovine serum albumin (BSA) marker, expressed as a percentage. SD values were scaled by the same marker mean. Cells highlighted in green indicate mean relative fluorescence intensities of 100% or higher. The table provides quantitative glycan-array binding signals and does not represent dissociation constants (*Kd*).

Suppl. Table S3

Molecular masses and oligomeric assemblies of recombinant hRTLs determined by native mass spectrometry and SDS-PAGE.

	Major monomer	Major dimer	Tetramer	HMW species
	Da	Da	Da	Detected by SDS-PAGE
hRTL-1	16,493-16,837	32,067-33,980	-	Yes
hRTL-2	16,342-16,652	32,065-35,332	CID confirmed	Yes
hRTL-3	17,332-17,411	34,124-34,744	-	-
hRTL-4	15,206-17,719	-	-	-
hRTL-5	-	30,271-30,986	61,084-61,795	-
hRTL-6	15,038-16,632	30,446-32,040	-	-

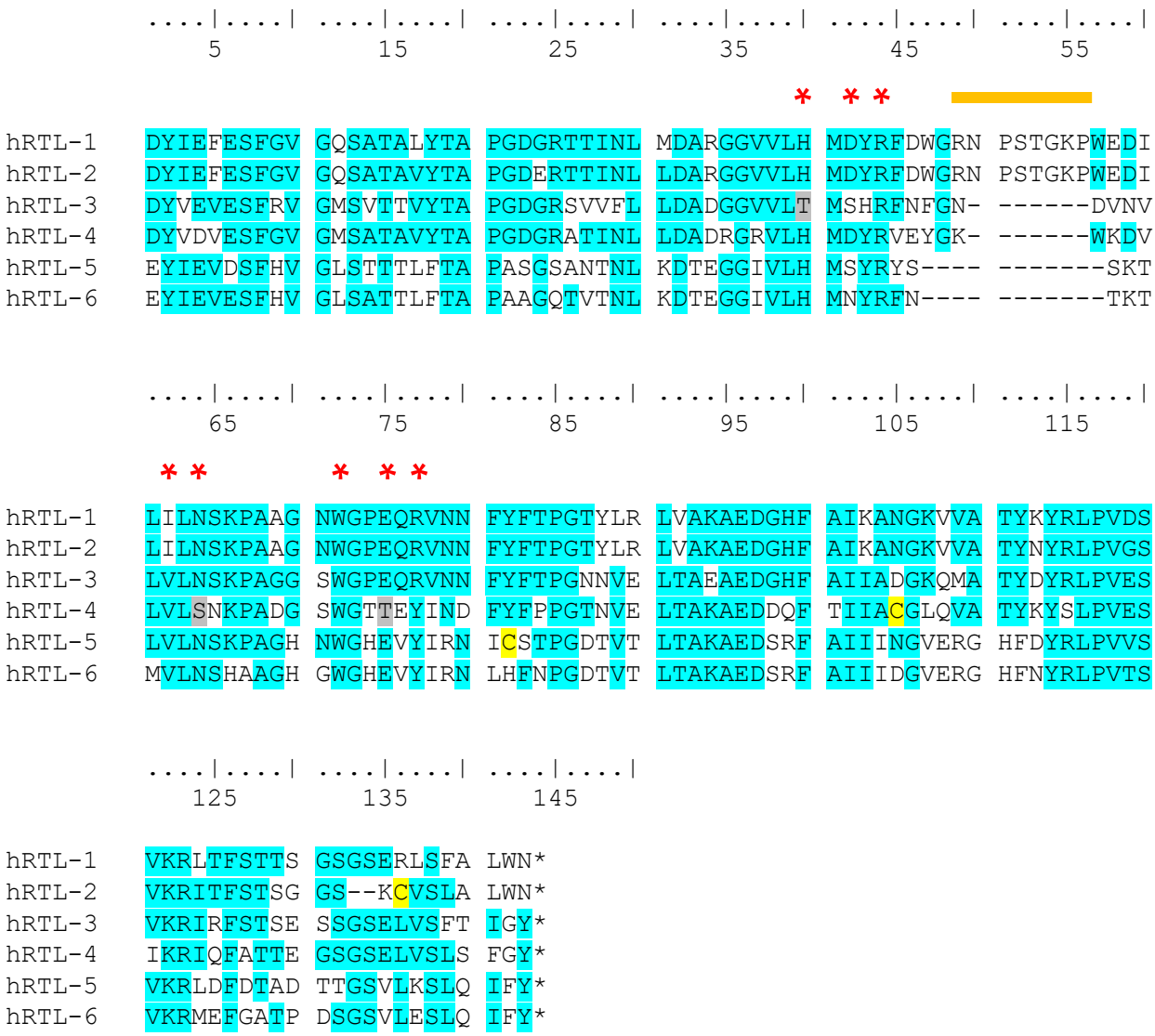
Coding DNA sequences (CDSs) of hRTL-1 to hRTL-6 used for recombinant protein expression.

hRTL-1 CDS	ATGAGCAAAATTAAAGGCAGCTCACATCATCATCACCATCATAGCAGCGGCCTGGTGCCGCGCGGCAGCCACGATTATATTGAATTTGAAAGCTTTGGCGTGGGCCAGA GCGCGACGGCGCTGTATACCGCGCCGGGCGATGGCCGCACCACCATTAATCTGATGGATGCGCGTGGCGGCGTCGTCCTGCATATGGATTATCGCTTTGATTGGGGCCG CAATCCGAGCACCGGTAAACCGTGGGAAGATATTCTGATTCTGAACAGCAAACCGGCCGCCGGCAATTGGGGCCCGGAACAGCGTGTGAACAATTTTTATTTCACCCCG GGTACGTACCTGCGCCTGGTGGCCAAAGCGGAAGATGGCCATTTTGCCATTAAAGCCAACGGCAAAGTGGTGGCGACCTACAAATATCGCCTGCCGGTGGATAGCGTTA AACGCCTGACCTTCAGCACCACCAGCGGCAGCGGCAGCGAACGTCTGAGCTTTGCGCTGTGGAACTAA*
hRTL-2 CDS	ATGAGCAAAATTAAAGGCTCGAGCCATCATCACCATCACCACAGCAGCGGCCTGGTGCCGCGCGGTTCGCACGATTATATTGAATTTGAAAGCTTTGGCGTGGGCCAGA GCGCGACCGCCGTGTATACCGCCCCGGGCGATGAACGCACCACGATTAACCTGCTGGATGCCCGCGGTGGCGTGGTGCTGCACATGGATTATCGTTTTGATTGGGGCCG CAACCCGAGCACGGGCAAACCGTGGGAAGATATTCTGATTCTGAACTCGAAACCGGCGGCGGGCAACTGGGGCCCGGAACAGCGCGTGAACAATTTTTATTTCACCCCG GGCACCTATCTGCGCCTGGTTGCGAAAGCGGAAGATGGCCATTTCGCGATTAAAGCCAACGGCAAAGTGGTGGCCACCTATAATTATCGCCTGCCGGTTGGCAGCGTGA AACGTATTACCTTTAGCACGAGCGGCGGCAGCAAATGTGTGAGCCTGGCGCTGTGGAATTAA*
hRTL-3 CDS	ATGAGCAAAATTAAAGGCTCAAGCCATCATCATCATCATCATAGCAGCGGCCTGGTGCCGCGCGGCAGCCACGATTACGTGGAAGTGGAATCTTTTCGCGTGGGCATGA GCGTGACCACCGTGTATACCGCGCCGGGCGATGGCCGCAGTGTGGTGTTTCTGCTGGATGCGGATGGCGGCGTCGTGCTGACCATGAGCCATCGCTTTAACTTTGGCAA TGATGTGAACGTTCTGGTGCTGAACAGCAAACCGGCGGGCGGCAGTTGGGGCCCGGAACAGCGCGTGAATAATTTTTATTTTACCCCGGGCAACAACGTGGAACTGACC GCCGAAGCCGAAGATGGCCATTTTGCGATTATTGCGGATGGCAAACAGATGGCGACCTACGATTATCGTCTTCCGGTGGAAAGCGTGAAACGCATTCGCTTTAGCACGA GCGAAAGCAGCGGTAGCGAACTGGTGAGCTTTACCATCGGCTACTAA*
hRTL-4 CDS	ATGAGCAAAATTAAAGGTAGCAGCCACCATCACCACCACCATAGCTCGGGCCTGGTGCCGCGTGGCAGCCATGATTACGTGGATGTTGAATCTTTTGGCGTGGGCATGA GCGCGACCGCGGTGTATACCGCCCCGGGCGATGGCCGTGCGACCATTAATCTGCTGGATGCGGATCGCGGCCGCGTGCTGCATATGGATTATCGCGTGGAATACGGTAA ATGGAAAGACGTTCTGGTGCTGAGCAACAAACCGGCCGATGGCAGCTGGGGCACCACCGAATATATTAACGATTTCTATTTTCCGCCGGGCACCAATGTGGAACTGACC GCCAAAGCCGAAGATGATCAGTTCACCATTATTGCGTGCGGCTTACAGGTGGCCACCTACAAATATAGCCTGCCGGTGGAAAGCATTAAACGTATTCAGTTCGCCACCA CCGAAGGTAGCGGCAGCGAACTGGTGAGCCTGAGCTTTGGCTATTAA*
hRTL-5 CDS	ATGAGCAAAATTAAAGGCAGCAGTCACCATCATCATCATCATAGCAGCGGCCTGGTGCCGCGCGGCAGCCATGAATATATTGAAGTGGATAGCTTTCATGTGGGCCTGA GCACAACCACCCTGTTCACCGCACCGGCGAGCGGCAGCGCCAACACCAATCTGAAAGATACCGAAGGCGGCATTGTGCTGCATATGAGCTATCGTTATTCAAGTAAAAC CCTGGTGCTGAACAGCAAACCGGCCGGCCACAACTGGGGCCACGAAGTGTATATTCGCAACATTTGTAGCACCCCGGGCGATACCGTGACCCTGACCGCCAAAGCCGAA GATAGCCGCTTTGCGATTATTATCAACGGCGTGGAACGTGGCCACTTTGATTATCGCCTGCCGGTGGTGAGCGTGAAACGTCTGGATTTTGATACCGCGGATACCACCG GTAGCGTGCTGAAAAGCCTGCAGATTTTTTATTAA*
hRTL-6 CDS	ATGAGCAAAATTAAAGGCAGCAGTCACCATCATCATCATCATAGCAGCGGCCTGGTGCCGCGCGGCAGCCATGAATATATTGAAGTGGAAAGCTTTCATGTGGGCCTGA GCGCGACCACCCTGTTCACCGCACCGGCGGCGGGCCAGACCGTCACCAATCTGAAAGATACCGAAGGCGGCATTGTGCTGCATATGAATTATCGTTTTAACACGAAAAC CATGGTGCTGAACAGCCATGCCGCCGGCCACGGCTGGGGCCACGAAGTGTATATTCGCAACCTGCATTTTAATCCGGGCGATACCGTGACCCTGACCGCCAAAGCCGAA GATAGCCGCTTTGCGATTATTATCGATGGCGTGGAACGTGGCCACTTTAATTATCGCCTGCCGGTGACCAGCGTGAAACGTATGGAATTTGGCGCGACCCCGGATAGCG GTAGCGTGCTGGAAAGCCTGCAGATTTTTTATTAA*

Suppl. Table S5

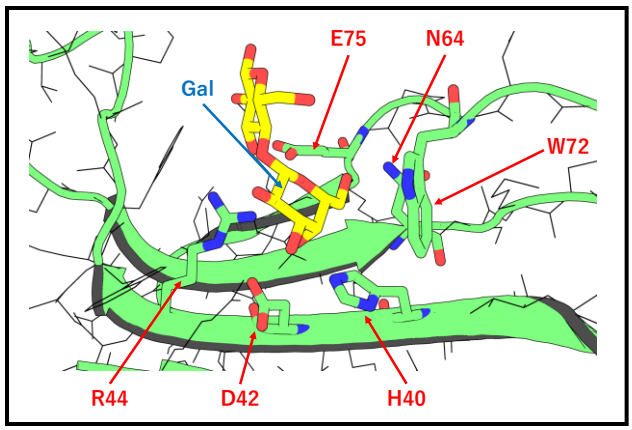
Amino acid sequences of hRTL-1 to hRTL-6 used as input for AlphaFold3 structure prediction.

hRTL-1	DYIEFESFGVGQSATALYTAPGDGRTTINLMDARGGVVLHMDYRFDWGRNPSTGKPWEDILILNSKPAAGNWGP EQRVNNFYFTPGTYLRLVAKAEDGHFAIKANGKVVATYKYRLPVDSVKRLTFSTTSGSGSERLSFALWN*
hRTL-2	DYIEFESFGVGQSATAVYTAPGDERTTINLLDARGGVVLHMDYRFDWGRNPSTGKPWEDILILNSKPAAGNWGP EQRVNNFYFTPGTYLRLVAKAEDGHFAIKANGKVVATYNYRLPVGSVKRITFSTSGGSKCVSLALWN*
hRTL-3	DYVEVESFRVGMSVTTVYTAPGDGRSVVFLLDADGGVVLTMSHRFNFGNDVNVLVLNSKPAGGSWGPEQRVNNF YFTPGNNVELTAEAEDGHFAIIADGKQMATYDYRLPVESVKRIRFSTSESSGSELVSFTIGY*
hRTL-4	DYVDVESFGVGMSATAVYTAPGDGRATINLLDADRGRVLHMDYRVEYGKWKDVLVLSNKPADGSWGTTEYINDF YFPPGTNVELTAKAEDDQFTIIACGLQVATYKYSLPVESIKRIQFATTEGSGSELVSLSFGY*
hRTL-5	EYIEVDSFHVGLSTTTLFTAPASGSANTNLKDTEGGIVLHMSYRYSSKTLVLNSKPAGHNWGHEVYIRN ICSTPGDTVTLTAKAEDSRFAIIINGVERGHFDYRLPVVSVKRLDFDTADTTGSVLKSLQIFY*
hRTL-6	EYIEVESFHVGLSATTLFTAPAAGQTVTNLKDTEGGIVLHMNYRFNTKTMVLNSHAAGHGWGHEVYIRN LHFNPGDTVTLTAKAEDSRFAIIIDGVERGHFNYRLPVTSVKRMEFGATPDSGSVLESLQIFY*

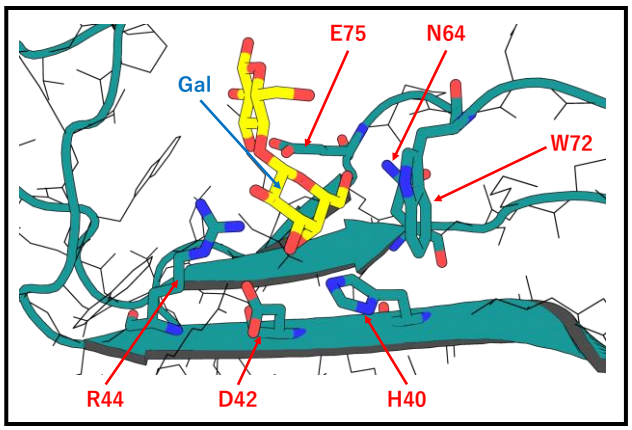


Supplementary Figure S1. **Amino acid sequence alignment of the six recombinant hRTLs.** Predicted signal peptide sequences [11] were omitted, and only the mature recombinant protein sequences were included in the alignment. Conserved residues are highlighted in cyan. Extra loops are indicated by orange bars. The consensus sequence of galectins involved in carbohydrate recognition is marked with red asterisks. Gray highlights indicate amino acids that deviate from the consensus sequence. Cysteine residues are highlighted in yellow.

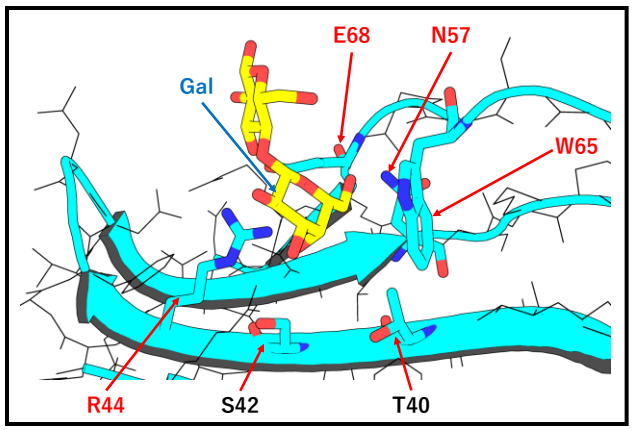
hRTL-1



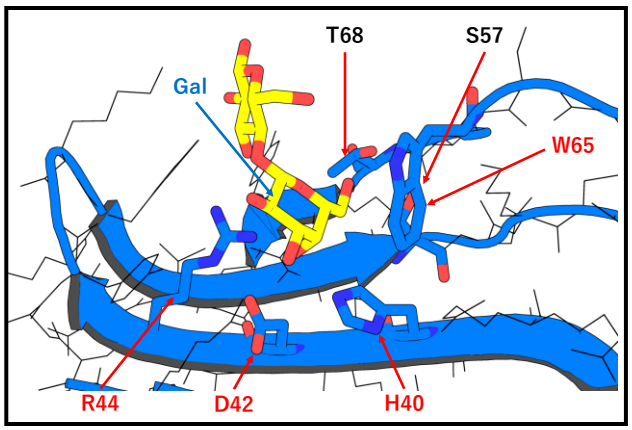
hRTL-2



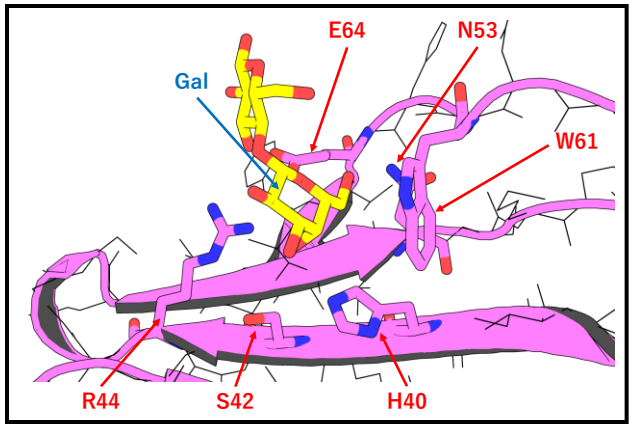
hRTL-3



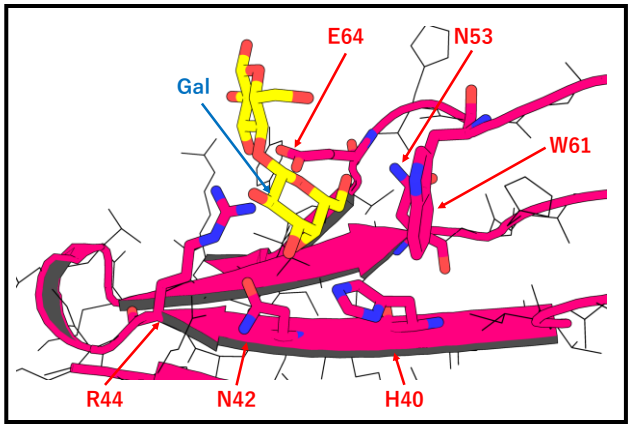
hRTL-4



hRTL-5

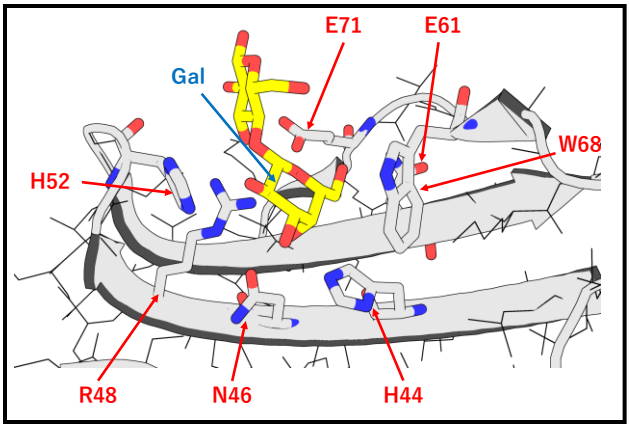


hRTL-6

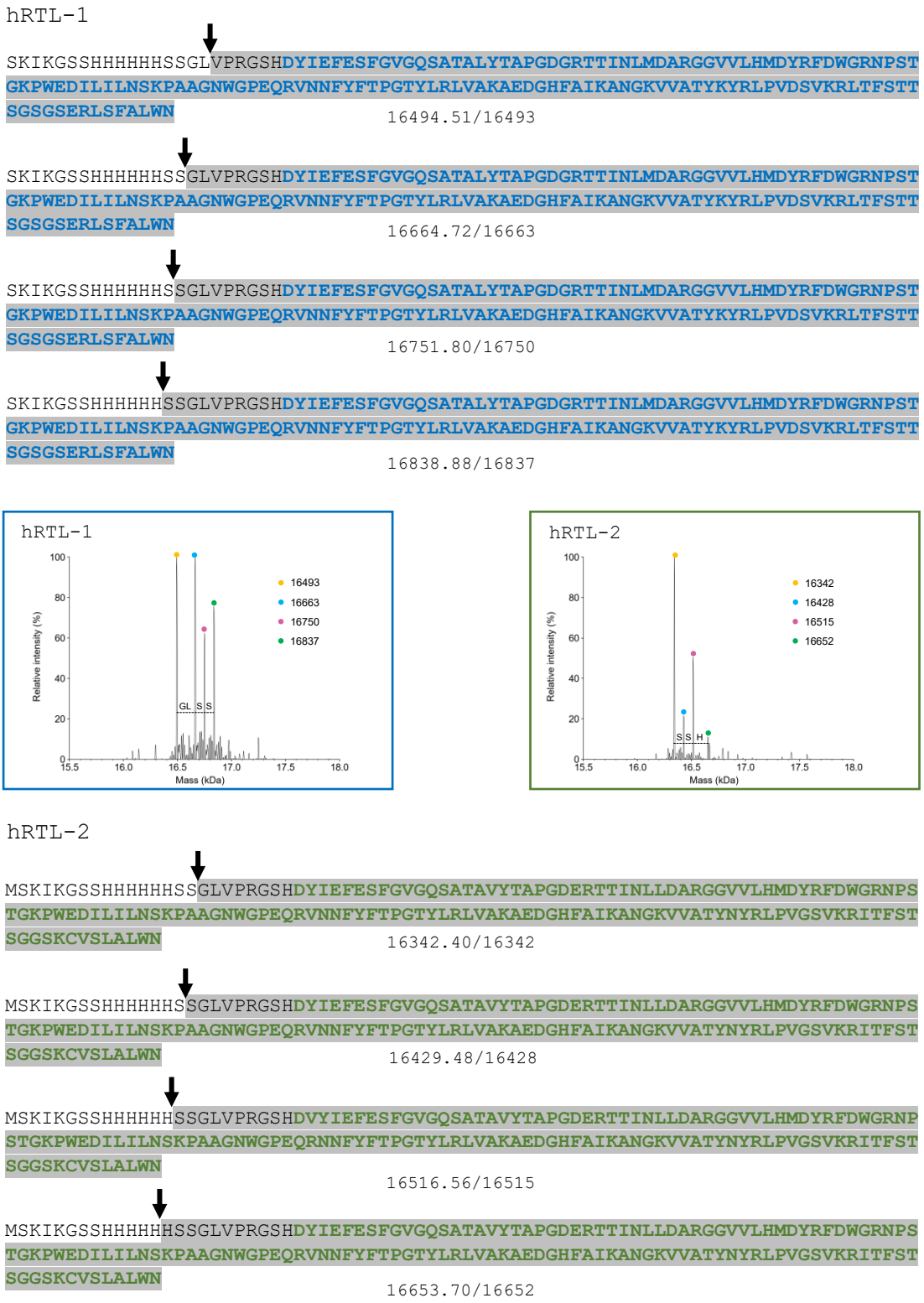


Supplementary Figure S2. Structural comparison of the carbohydrate-binding sites of hRTLs and human galectin-1. (Legend on the following page.)

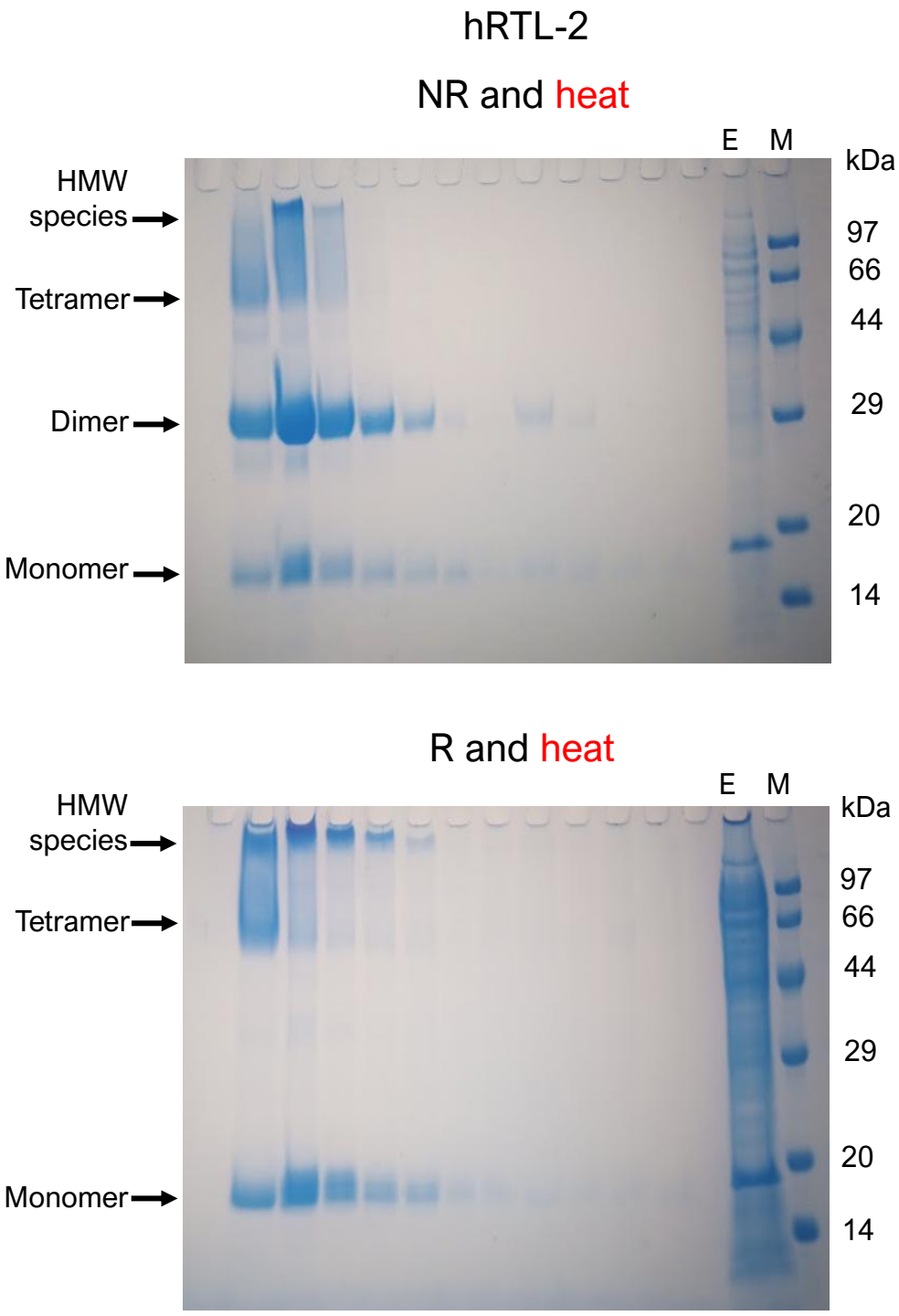
Human Gal-1



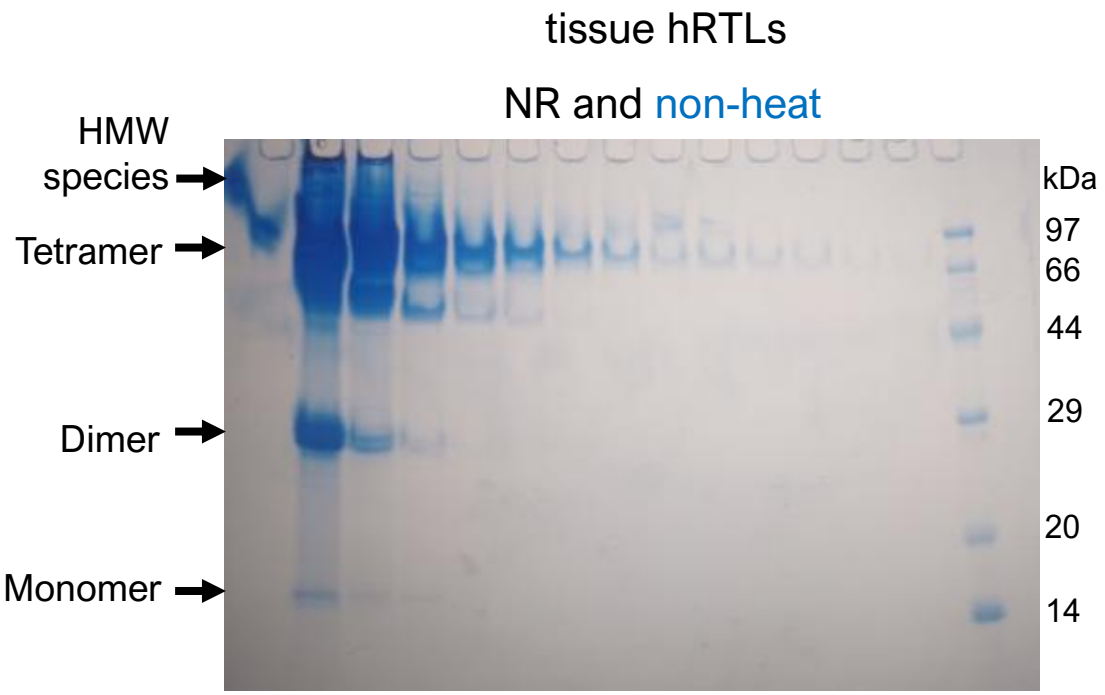
Supplementary Figure S2. **Structural comparison of the carbohydrate-binding sites of hRTLs and human galectin-1.** Structural models of hRTL-1 to hRTL-6 were compared with human galectin-1 (PDB 1W6O) around the predicted carbohydrate-binding sites. The structures are shown as ribbon representations, with residues surrounding the carbohydrate-binding sites labeled by amino acid type and residue number. The galactose moiety of lactose is indicated in blue (Gal). The comparison highlights conserved and substituted residues within the ligand-binding region of the hRTLs. Residues that differ from the corresponding conserved residues in the other hRTLs are shown in black: Thr40 and Ser42 in hRTL-3, and Ser57 and Thr68 in hRTL-4.



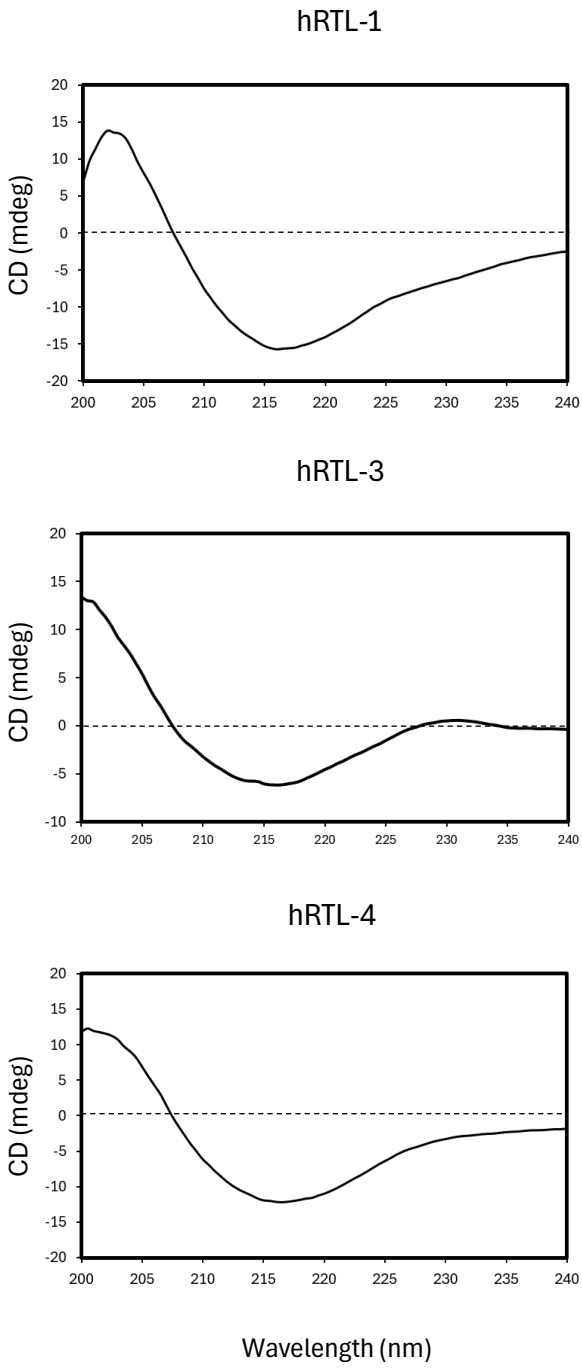
Supplementary Figure S3. **Assignment of monomeric mass variants of recombinant hRTL-1 and hRTL-2.** Multiple monomeric species detected by native mass spectrometry were assigned to theoretical molecular masses calculated from alternative N-terminal processing of the recombinant proteins. The observed masses closely matched the calculated values, indicating that the mass heterogeneity arises from differential retention of the N-terminal expression-derived sequence rather than from post-translational modification. Arrows indicate cleavage sites. Bold letters represent the mature hRTL sequences. Numbers indicate the theoretical and experimentally determined molecular masses (theoretical/experimental, Da).



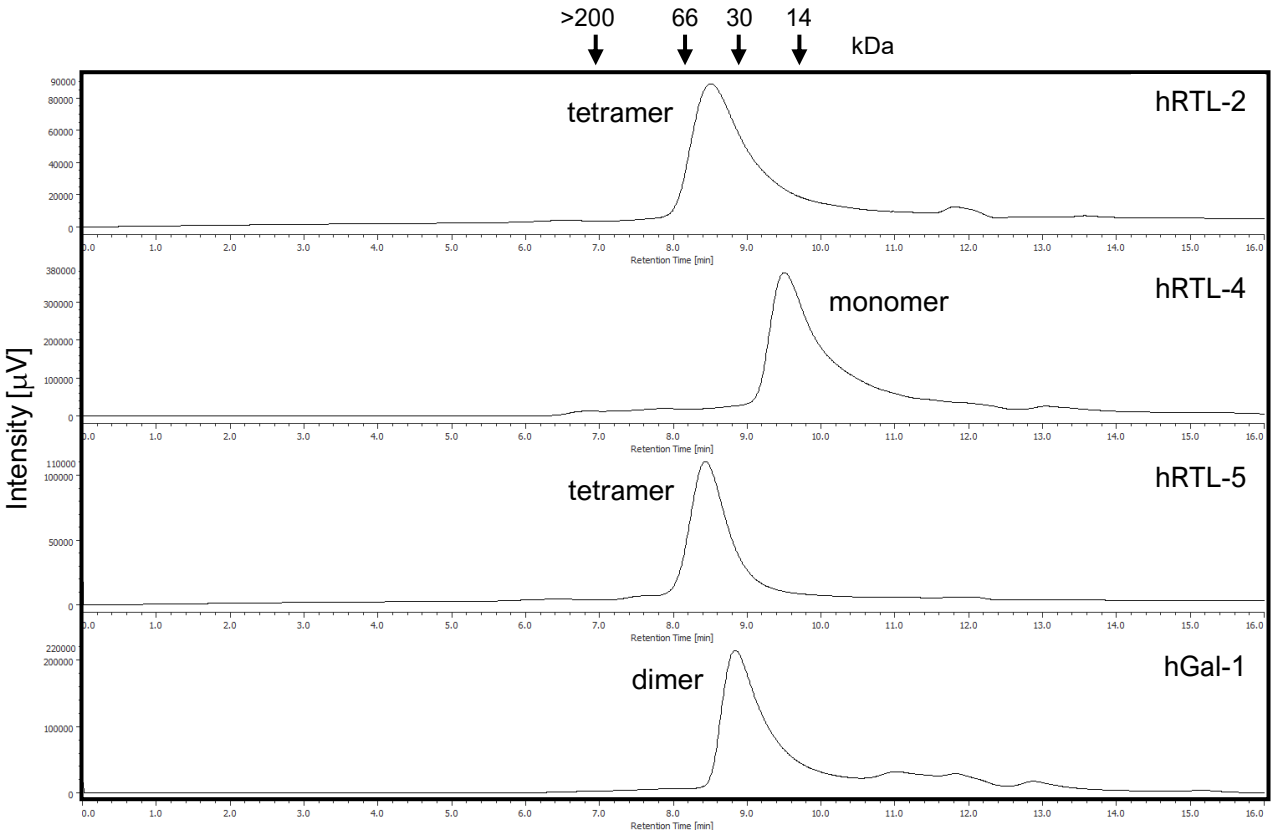
Supplementary Figure S4. Heated SDS-PAGE analysis of recombinant hRTL-2 under non-reducing and reducing conditions. Heated SDS-PAGE analysis of recombinant hRTL-2 under non-reducing (NR) and reducing (R) conditions. Recombinant hRTL-2 was heated in SDS sample buffer in the absence (upper panel) or presence (lower panel) of reducing reagent prior to electrophoresis. Protein samples were serially diluted from left to right. The positions of monomer, dimer, tetramer, and higher-molecular-weight species (HMW species) are indicated. These original gel images correspond to the cropped images shown in Fig. 5B. Crude extraction of recombined bacteria (E). Molecular markers (M).



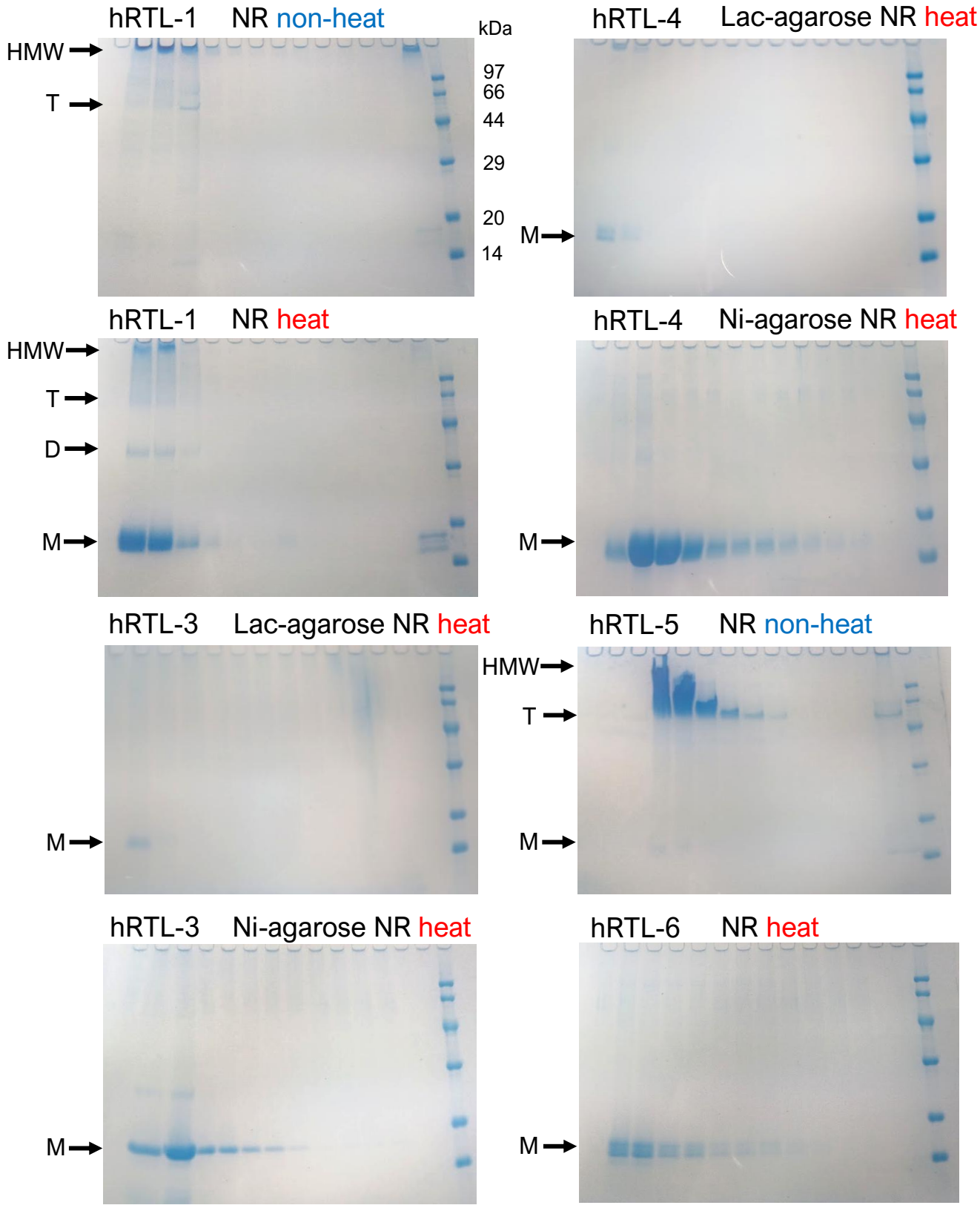
Supplementary Figure S5. **Assemblies of native hRTLs purified from the demosponge *Chondrilla australiensis*.** Sponge tissues (10 g) were homogenized in sodium bicarbonate buffer, and the supernatant was applied to a lactose–agarose affinity column. After washing with the same buffer, bound hRTLs were eluted with buffer containing 200 mM lactose [11]. Eluted fractions were analyzed by non-heated SDS-PAGE under non-reducing conditions. The positions of monomers, dimers, tetramers, and higher-molecular-weight species (HMW species) are indicated.



Supplementary Figure S6. **Far-UV CD spectra of recombinant hRTL-1, hRTL-3, and hRTL-4.** Far-UV circular dichroism (CD) spectra were measured for recombinant hRTL-1, hRTL-3, and hRTL-4. All three proteins exhibited similar overall spectral features, including a pronounced negative band around 215–220 nm, consistent with predominantly β-sheet-rich secondary structures. The similar overall spectral characteristics of hRTL-3 and hRTL-4 to those of hRTL-1 argue against gross protein misfolding as the primary explanation for their markedly reduced glycan-binding activity.

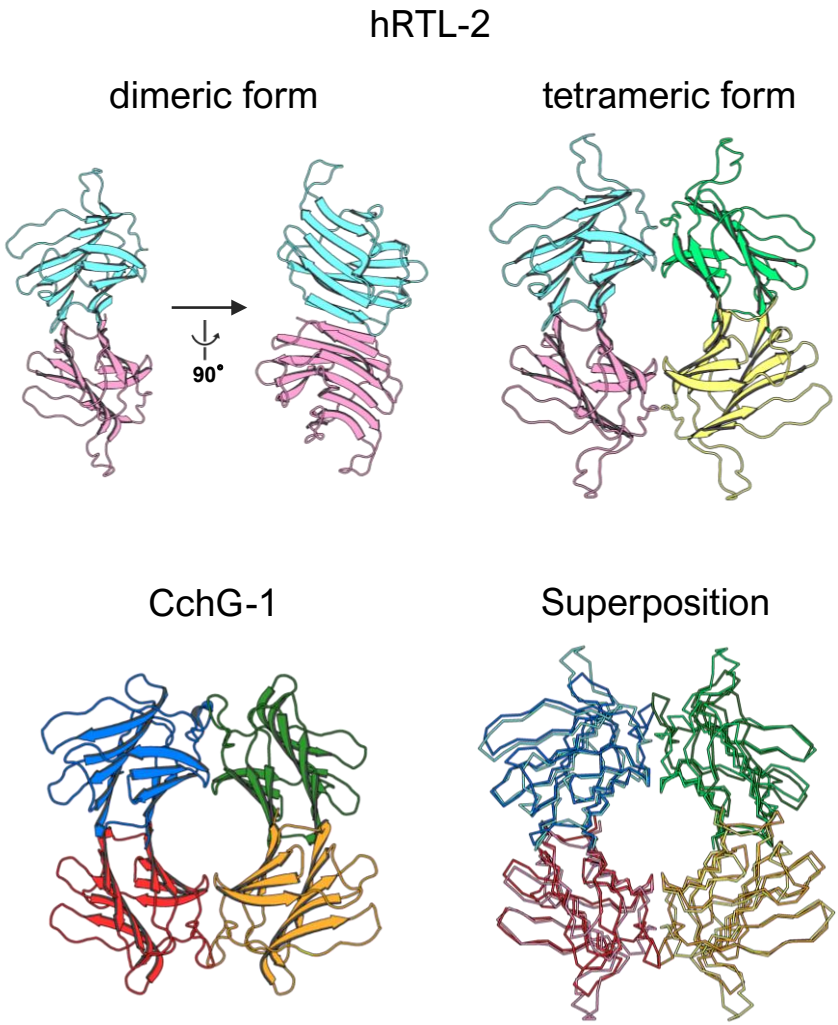


Supplementary Figure S7. **Size-exclusion chromatography of recombinant hRTL-2, hRTL-4, hRTL-5, and human galectin-1.** Purified recombinant hRTL-2, hRTL-4, and hRTL-5, together with human galectin-1 (hGal-1), were analyzed by size-exclusion chromatography. Molecular mass standards are indicated above the chromatograms: blue dextran (>200 kDa), bovine serum albumin (66 kDa), carbonic anhydrase (30 kDa), and horse myoglobin (14 kDa). The major peaks of hRTL-2 and hRTL-5 eluted at positions corresponding approximately to 66 kDa, consistent with tetrameric assemblies, whereas hRTL-4 eluted at a position corresponding approximately to the monomeric molecular mass. Human galectin-1 (hGal-1) eluted at a position consistent with its dimeric state.



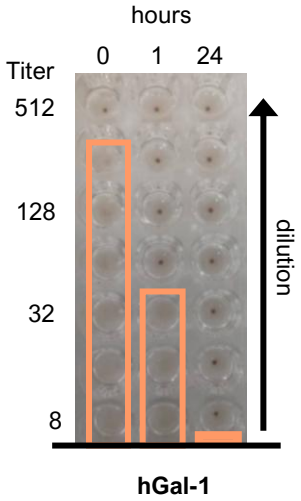
Supplementary Figure S8. Representative SDS-PAGE analyses of recombinant hRTLs. (Legend on the following page.)

Supplementary Figure S8. Representative SDS-PAGE analyses of all recombinant hRTLs except hRTL-2. Recombinant hRTL-1, hRTL-3, hRTL-4, hRTL-5, and hRTL-6 were analyzed under the indicated conditions. hRTL-1, hRTL-5, and hRTL-6 were examined under non-reducing (NR) conditions with or without heat treatment (non-heat or heat). hRTL-3 and hRTL-4 were analyzed after purification by lactose-agarose or Ni-agarose chromatography under non-reducing conditions. Representative molecular species are indicated as HMW (higher-molecular-weight species), T (tetramer), D (dimer), and M (monomer). Molecular mass markers (kDa) are shown on the right. These representative gel images correspond to the recombinant proteins used throughout this study.



Supplementary Figure S9. Predicted oligomeric models of hRTL-2 and comparison with the tetrameric structure of CchG-1. Predicted dimeric and tetrameric models of hRTL-2 are shown in comparison with the experimentally determined tetrameric structure of CchG-1. The predicted dimeric form of hRTL-2 is shown in two orientations related by a 90° rotation. The predicted tetrameric form of hRTL-2 is shown at the upper right, and the experimentally determined tetrameric structure of CchG-1 is shown at the lower left (PDB ID: 4AGV) [12]. The superposition of the predicted hRTL-2 tetramer and the CchG-1 tetramer is shown at the lower right, with an RMSD of 2.85 Å over 264 aligned residues.

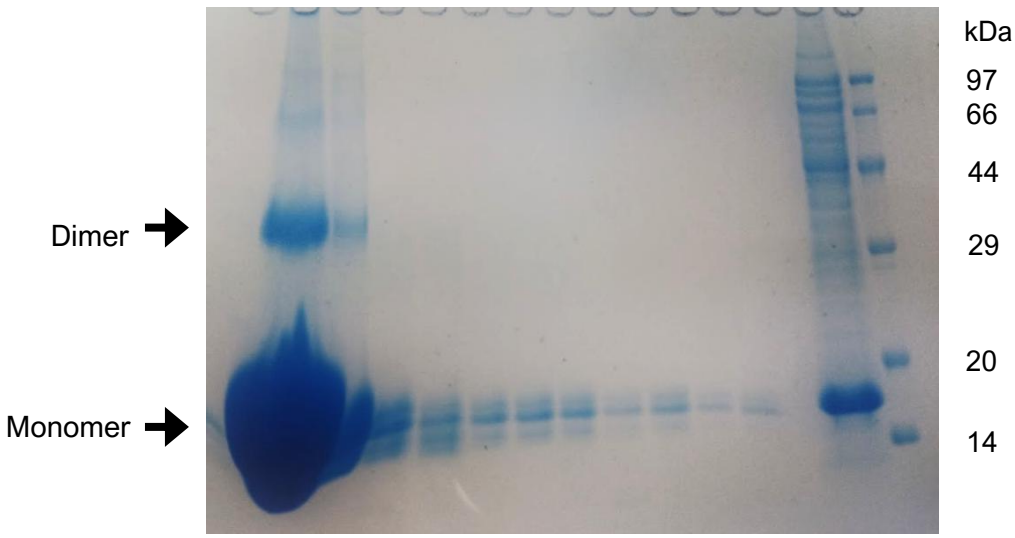
A.



B.

MASGLVASNLNLKPGESLRVRGEVAPDAKSFVLNLGKDSNNLSLH
FNPRFNAHGDANTIVSNSKDGGAWGTEQREAVFPFQPGSVAEVSI
TFDQANLTVKLPDGYEFKFPNRLNLEAINYMAADGDFKIKSVAFD

C.



Supplementary Figure S10. Thermal stability of human galectin-1 (hGal-1) assessed by a hemagglutination assay. hGal-1 was incubated at 60°C for 0, 1, and 24 h. Hemagglutination titers (reciprocal dilution; y-axis) were normalized to the initial value (256) (A). Primary structure of recombinant hGal-1. All six original cysteines in the polypeptide were substituted by serine residues (green highlights) (B). The purity of the recombinant hGal-1 (C).